Macromolecular Research, Vol. 17, No. 7, pp 476-482 (2009)

Influence of Amorphous Polymer Nanoparticles on the Crystallization Behavior of Poly(vinyl alcohol) Nanocomposites

Kyung Jin Lee, Jihye Lee, Jin-Yong Hong, and Jyongsik Jang*

School of Chemical and Biological Engineering, College of Engineering, Seoul National University, Seoul 151-742, Korea

Received August 19, 2008; Revised December 3, 2008; Accepted December 4, 2008

Abstract: The crystallization behavior of poly(vinyl alcohol) (PVA) in the presence and absence of polypyrrole nanoparticles (PPy NPs) was investigated in terms of the heterogeneous nucleation effect of PPy NPs using FTIR, X-ray diffraction, differential scanning calorimeter and polarized optical microscope analysis. PPy NPs were prepared by dispersion polymerization method stabilized by PVA in aqueous solution. A polymer nanocomposite with uniform dispersity could be readily obtained due to the enhanced compatibility between the filler and matrix. Compared with the PPy NP-absent PVA, the PPy NP/PVA nanocomposite exhibited an enhanced degree of crystallinity. The degree of crystallinity increased up to 17% at the PPy NP concentration of 1 wt%, compared to the pristine PVA. The PPy NP acted as an effective nucleating agent during the crystallization process, thereby enhancing the degree and rate of crystallization. The kinetics study of the crystallization also revealed the decreased value of the Avrami coefficient in the case of the PPy NP/PVA nanocomposite.

Keywords: semicrystalline polymer, nanocomposite, fourier transform infrared spectroscopy, polypyrrole nanoparticle, poly(vinyl alcohol).

Introduction

Crystallization behavior of semicrystalline polymer has been extensively investigated due to their technological and theoretical importance. Diverse semicrystalline polymers such as polyethylene (PE), polypropylene (PP), polyamide, poly(ethylene terephthalate) (PET), and polystyrene (PS) have been adopted to analyze the crystallization behavior of polymeric materials.[1-5] Crystallization behavior of poly(vinyl alcohol) (PVA) has been also studied by several research groups under different experimental conditions, because the hydroxyl group containing semi-crystal polymers have been of special interest.[6-15] In general, these studies have been conducted using differential scanning calorimeter (DSC), X-ray diffraction scattering (XRD), Fourier transform infrared spectroscopy (FTIR) and polarizing optical microscopy (POM).[6-18]

Recently, together with the advances of nanotechnology, the crystallization behavior of polymer nanocomposites have been scrutinized to expand their application fields.[19-21] Various nanomaterials such as montmorillonite,[22-24] silica,[25-28] carbon nanotube (CNT),[28-30] and POSS[31] were blended with the semicrystalline polymer. However, it is still challenging task to prepare the nanocomposite with reasonable dispersity due to the poor compatibility between the inorganic filler and the organic matrix. Ke *et al.* focused on the surface treatment of silica nanoparticle with PS in order to enhance the compatibility between SiO_2 and PET.[32] They reported that the PS treated-silica could be more uniformly dispersed in PET matrix. When the nanofillers are composed of organic materials, the monodisperse polymer nanocomposite can be readily obtained due to the enhanced compatibility between organic nanofiller and polymer matrix, leading to the efficient nucleation in crystallization process. However, there is limited information to study the crystallization behavior of polymer nanoparticle (NP)/semicrystalline polymer nanocomposite. In general, crystallization behavior of polymer-polymer system has been conducted with the blend of amorphous polymer-crystalline polymer.[33-35] When the amorphous polymer was added into the crystalline polymer, the degree of crystallinity decreased with increasing the amount of amorphous portion.[33,34,36]

Herein we report the crystallization behavior of polypyrrole nanoparticles(PPy NPs)/PVA nanocomposite using FTIR, XRD, DSC and POM analysis in the view point of the role of PPy NPs. The degree of crystallinity of nanocomposite enhanced with increasing the contents of PPy up to 1 wt%, differently with the bulk PPy/PVA composite. Judging from the FTIR analysis and crystallization kinetics based on the DSC thermogram, it is revealed that the PPy NPs can play a role in an effective nucleating agent in crystallization process of PVA. POM and XRD scattering analysis are also

*Corresponding Author. E-mail: jsjang@plaza.snu.ac.kr

performed in order to confirm the crystallization behavior of pristine PVA and PPy/PVA nanocomposite.

Experimental

Materials. Poly(vinyl alcohol) (98~99% hydrolyzed, Mw: 31,000~50,000) was used as a crystalline polymer. Pyrrole and Iron (III) chloride were used as monomer and oxidant in order to prepare PPy nanoparticles(PPy NPs). All of chemicals were purchased from Aldrich Co. and used as received.

Synthesis of Polypyrrole Nanoparticles. PPy NPs as a nanofiller were prepared by dispersion polymerization with PVA stabilizer, which was well established by Armes *et al.*.[37-39] At first, the stabilizer (PVA) was dissolved in distilled water, and the mixture was stirred at 25 °C. The concentration of PVA to distilled water was fixed at 0.83 wt%. The $FeCl_3$ (0.137 mol) as an oxidative initiator were added into PVA aqueous solutions. After a few minutes to allow equilibration, pyrrole as a monomer was introduced into the system. The volume ratio of pyrrole-to-water was 6.67×10^{-3}. Polymerization occurred immediately and the color of the solution turned into black within few minutes. The solution was stirred for at least 2 h for sufficient polymerization. The PPy NPs were separated by centrifugal force, and washed three times with water to remove impurities, and residual PVA. Finally, the PPy NPs were obtained by drying the solution in vacuum at room temperature for 24 h.

The bulk PPy for control experiment was fabricated by dispersion polymerization without PVA stabilizer. The oxidant was dissolved in aqueous solution (0.137 mol) and the pyrrole monomer was added into the $FeCl_3$ solution. The color of solution tuned from yellow to black, immediately, and the polymerization performed for 2 h. The distilled water was poured into the solution to remove residual reactant, and the PPy was precipitated.

Preparation of PPy/PVA Nanocomposite. PPy NPs with various contents were dispersed by sonication for 10 min in 10 mL of distilled water at room temperature. The PPy NPs prepared with PVA stabilizer can be readily redispersable to water.[40] Then, the PVA of 10 wt% against distilled water was introduced into the PPy NPs/aqueous solution, and the mixture was stirred for 1 h at 75 °C. PPy NP/PVA composite thin films were prepared by casting method using imide film at 90 °C drying oven. The compositions of PPy NP/PVA nanocomposite were 0.5/99.5, 1/99, 2.5/97.5, 5/95, and 8/92 wt%, respectively. Although small amount of PVA can remain on the surface of PPy NPs, this amount might be negligible. Therefore, final weight ratio of PPy NP to PVA can be controlled by adjusting initial amount of PPy and PVA.

Crystallization Procedure of PVA and Nanocomposite. The PVA film in presence or absence of PPy NPs obtained by solvent casting was located between the KBr windows. These specimens were heated up to meting temperature of PVA (240 °C) and pressed under 10,000 pound using hot-press. The amorphous PVA films were obtained by quenching in acetone and heat treated as a function of annealing time at different temperatures (100, 120, and 150 °C). Isothermal crystallization behaviors of PPy NP/PVA nanocomposite were evaluated by FTIR analysis. FTIR spectra were measured to observe the crystallization behavior of PPy/PVA nanocomposite.

The samples for XRD analysis were prepared as follow. At first, pristine PVA solution and PPy(1 wt%)/PVA solution were dried at 90 °C and the films were melted on imide film at 240 °C for 10 min in order to remove the thermal history, and then quenched in acetone at 3 °C. The two types of film such as pristine PVA and PPy (1 wt%)/PVA film were annealed at 120 °C for 20 min.

The differential scanning calorimetry (DSC) analysis was performed for analyzing non-isotherm crystallization behavior of PVA and Ppy/PVA nanocomposite under nitrogen flow. The samples were heated to melting point of PVA (~240 °C) at a heating rate of 20 °C/min and kept at 240 °C for 10 min in order to remove thermal history. Then, the samples were cooled down to room temperature at a cooling rate of 10 °C/min.

Instrumental Analysis. The FE-SEM (Field Emission Scanning Electron Microscope) and TEM (Transmission Electron Microscope) images were taken with a JEOL 6330F microscope and JEOL 2000FX analytical microscope. SEM images were obtained from the powder state of PPy NPs. The TEM images of PPy NP/PVA composites were taken by casting highly diluted PVA/PPy solution onto copper grid in order to obtain monolayer PVA film. FTIR spectra were recorded on a Bomem MB 100 FTIR spectrometer within the range between 1600 and 700 cm^{-1} and obtained over 32 scans in absorbance mode at resolution of 2 cm^{-1}. Wide angle X-ray scattering analysis was performed on a General Area Detector Diffraction System (GADDS) with a generator voltage of 40 kV and a current of 45 mA. DSC analysis was carried out on a Perkin Elmer DSC-7.

Results and Discussion

Figure 1(a) shows the SEM image of PPy NP prepared by dispersion polymerization with PVA stabilizer. The particle size of PPy NP is measured to be about 50 nm with reasonable uniformity and spherical shape. In addition, there is no particular aggregation of PPy nanoparticle even after water evaporation.[37-39] The electronic diffraction (ED) pattern (inset in Figure 1(a)) and the X-ray powder diffraction (Figure 1(c)) presented that the PPy NPs were amorphous polymer. The PPy NP/PVA film fabricated by simple casting method maintains their uniform dispersity, because the PPy NP can be readily redispersable in water, as illustrated in precedent works.[40] Figure 1(b) shows the PPy NP/PVA film whose PPy contents are fixed at 1 wt%. In order to prepare PVA thin films, the PVA/PPy NP solution was highly diluted and dried at

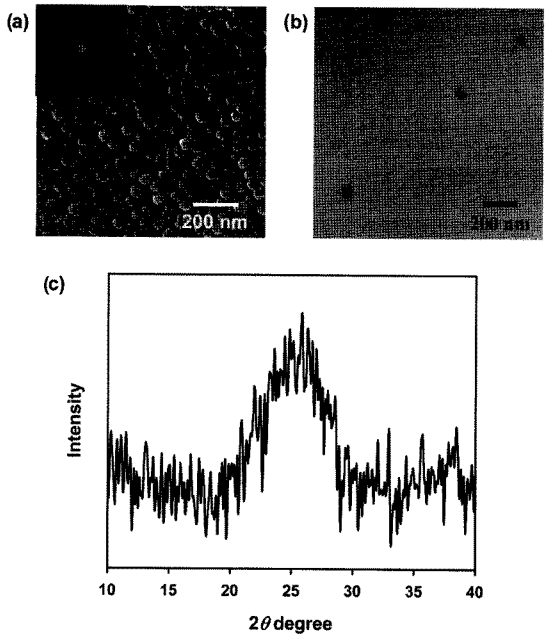

Figure 1. (a) SEM image of polypyrrole nanoparticle prepared by dispersion polymerization with PVA stabilizer (inset: ED pattern of PPy nanoparticle), (b) TEM image of PPy NP/PVA (1 wt%) nanocomposite (the arrow indicates PPy nanoparticle dispersed in PVA matrix) and (c) X-ray powder diffraction of PPy nanoparticles.

room temperature on copper grid. The TEM image presents that the PPy NPs (arrow) are well-dispersed in PVA films with reasonable particle-particle distance (400~600 nm) and this value is similar with the calculated mean distance (ca. 500 nm). Judging from SEM and TEM images, the PPy NP and PPy NP/PVA nanocomposite were successfully prepared by dispersion polymerization method and solution casting method without no particular particle aggregation and morphological deformation of PPy NPs.

Figure 2 presents the FTIR spectra of PVA (Figure 2(a)) and PPy NP/PVA-1 wt% (Figure 2(b)) annealed at 120 °C as a function of different annealing times. While these FTIR spectra demonstrate the characteristic peaks of PVA, there is a difference in peak intensity, which might be responsible for the change of crystallinity. The characteristic FTIR bands of PVA were summarized in Table I. Among them, the peak at 1140 cm^{-1} is strongly related with the crystalline phase.[6-11,43-45] It has been generally accepted that the change of crystalline phase is less influenced on the peak intensity of CH_2 deformation. Therefore, the peaks at 1427 or 850 cm^{-1} corresponding to in-plane deformation of CH_2 can be used as the internal standard to compare crystallinity of different samples. In this study, the peak at 850 cm^{-1} is selected as an internal standard.[9,10,41-43]

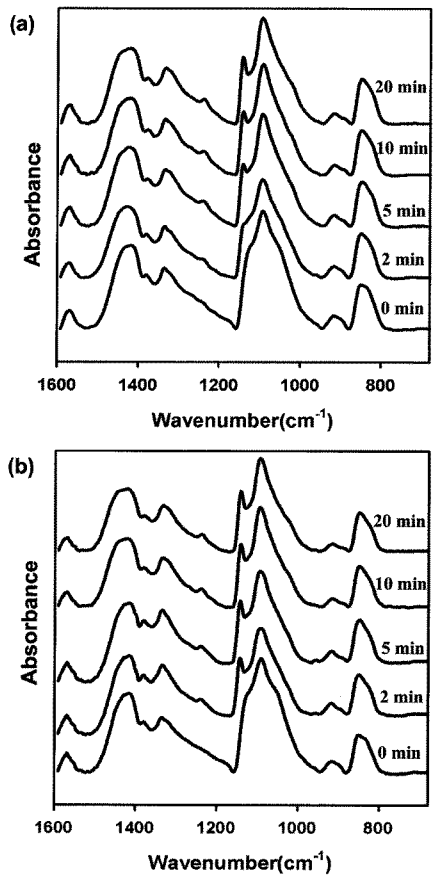

Figure 2. FTIR spectra of (a) PVA and (b) PPy NP/PVA nanocomposite as a function of different annealing time at 120 °C (0 min means the amorphous PVA without heat treatment).

Table I. Characteristic Infrared Peaks for PVA

Wavenumber (cm^{-1})	Band Assignment
3484	OH stretching
2938	CH_2 stretching
1653	C=C stretching
1427	CH_2 scissoring
1375, 1331	CH_2 deformation
1230	CH deformation
1140	C-O stretching (crystalline form)
1097	C-O stretching
916	C-C stretching
853	CH_2 rocking

At first, the peak intensity of 1140 cm^{-1} of PVA gradually increases with increasing heat treatment time (Figure 2(a)).

There are no bands at 1140 cm^{-1} in the amorphous PVA (without annealing), implying that amorphous PVA is successfully prepared by quenching process. The peak intensity of 1427 cm^{-1} had fixed value as a function of different annealing time, because the CH_2 deformation has no relation with the change of crystalline phase. In addition, the CH deformation peak at 1236 cm^{-1} appears in crystalline state (generally very weak intensity).[9,10,41-43]

In Figure 2(b), the FTIR spectra of PPy NP/PVA show the similar tendency with that of pristine PVA, but the C-O stretching at 1140 cm^{-1} is conspicuously enhanced compared with the pristine PVA. The PPy NP/PVA nanocomposite has higher degree of crystallinity than the pristine PVA. At 2 min annealing time, the enhancement of intensity ratio is obvious, implying that the PPy NPs act as a heterogeneous nucleating agent. It has been well established that the inorganic nanofillers such as silica, clay, and CNT act as a heterogeneous nucleating agent in crystalline polymer nanocomposite.[22-30] However, it is noteworthy that the nanosized amorphous polymer can play a similar role in the crystalline polymer composite. In addition, the relative peak intensity at 1236 cm^{-1} of PPy NP/PVA nanocomposite has also high values comparing to pristine PVA.

The control experimental was performed using bulk PPy in order to compare with the effect of NP on PVA crystallization. The bulk PPy was synthesized in ferric chloride aqueous solution without PVA stabilizer, and was mixed with the PVA matrix. Because the bulk PPy is synthesized without any stabilizing agent such as PVA and surfactant, no specific shapes are observed in bulk PPy. Figure 3 displays the intensity ratio of crystalline C-O peak to the internal standard of pristine PVA and PVA in the presence of bulk PPy and PPy NP. The prepared films were annealed at 120 °C for 20 min. The intensity ratio of C-O stretching to the internal standard is about 0.93, 0.92, and 1.11, respectively. The PPy NP/PVA nanocomposite has relatively higher degree of crystallinity than the pristine PVA. On the other hand, the bulk PPy/PVA composite shows similar degree of crystallinity with the pristine PVA. Because small amount of bulk PPy is added to the PVA matrix, the heterogeneous nucleating effect of bulk PPy is negligible. Provided that the amount of bulk PPy in the composite increased, the degree of crystallinity decreased due to the amorphous property of PPy. It is generally known that if the amorphous polymer is blended with the semicrystalline polymer, the degree of crystallinity decreases with increasing amount of amorphous polymer.[33,34,36] However, present study reveals that the amorphous nanoparticle can play a role in enhancing the crystallinity of matrix polymer.

The degree of crystallinity of PVA in the presence and absence of PPy nanoparticle is further confirmed by X-ray diffraction patterns. Figure 4 shows the XRD patterns of pristine PVA and PPy NP/PVA (1 wt%), before and after isotherm crystallization. It is generally known that there are broad XRD peak at amorphous phase, as shown in both XRD spectra of amorphous PVA in the presence and absence of PPy NPs. After isotherm crystallization, there is an intense peak appearing at 2θ=19.5° with the lattice distance of 4.55 Å.[44] The peak intensity of crystalline PPy NP/PVA (1 wt%) is higher than that of neat PVA and these results are well matched with the FTIR analysis.

Figure 5 shows the relative intensity of crystalline C-O peak to an internal standard as a function of PPy NP contents. In the concentration range of 0~1 wt%, the intensity ratio of crystalline C-O to the internal standard enhances with adding the more PPy NPs to the nanocomposite. How-

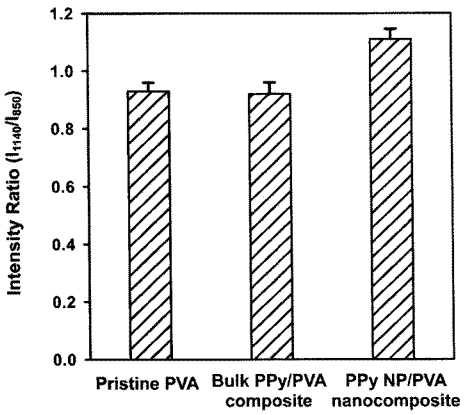

Figure 3. Intensity ratio of crystalline C-O peak (I_{1140}) to an internal standard (I_{850}) of pristine PVA, bulk PPy/PVA (1 wt%), and PPy NPs/PVA (1 wt %) nanocomposite (heat treatment at 120 °C for 20 min).

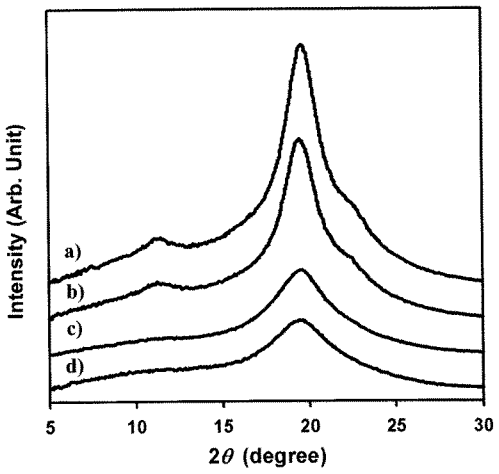

Figure 4. X-Ray diffraction patterns of amorphous and crystalline phase in PVA with different condition (a) crystalline PPy NP/PVA (1 wt%) nanocomposite, (b) crystalline PVA, (c) amorphous PPy NP/PVA nanocomposite (1 wt%), and (d) amorphous PVA.

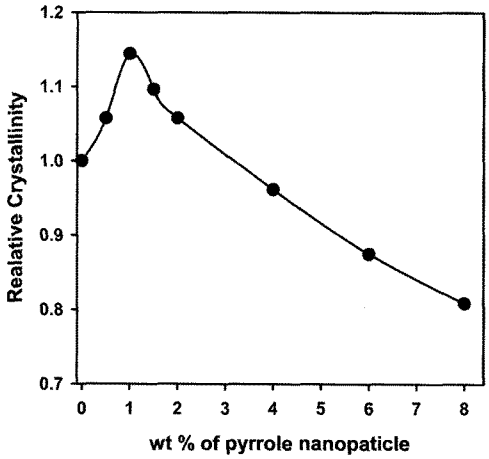

Figure 5. Relative crystallinity of PVA as a function of PPy nanoparticle contents.

ever, that is reduced when more PPy NPs (above 1 wt%) is added to the PVA. This could be ascribed to the physical hindrance of PPy NPs for the crystal growth. Although the PPy NP can be efficient nucleating agent at low concentration, the physical hindrance of PPy NPs prominently affect on the PVA crystallization at high concentration of PPy NPs. This result was well matched with the precedent report concerning the crystallinity behavior of other nanocomposite materials.[33,34,36]

Figure 6 shows the intensity ratio of crystalline C-O peak at 1140 cm^{-1} to the internal standard as function of annealing time at low PPy NP concentration. The intensity ratio enhances with increasing annealing time. In addition, as the

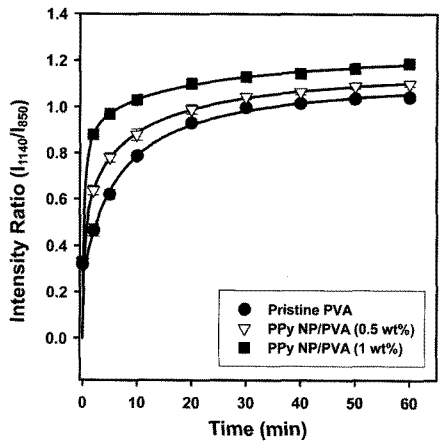

Figure 6. Intensity ratio of crystallized C-O peak (1140 cm^{-1}) to the internal standard of C-H stretching vibration (850 cm^{-1}) as a function of different crystallization time (crystallization temperature: 120 °C).

composition of PPy NP rises, the intensity ratio of PVA increases. This result can be direct evidence that the PPy NPs of below 1 wt% can enhance the degree of crystallinity. The intensity ratio of PPy NP/PVA nanocomposite (1 wt%) increases up to 17% compared to the pristine PVA at the 120 °C of annealing temperature. At the initial stage of crystallization process, the crystallinity increment of PPy NP/PVA composite film is more obvious comparing to the neat PVA. In this stage (Figure 5(a)), the nucleation effect is dominant to determine total crystallinity. Because the physical hindrance effect of PPy NPs is relatively insignificant, the crystallinity of PVA strongly depends on the initial nucleation activity. Accordingly, adding the PPy NP can make drastically increment of the crystallinity of PVA at initial stage (2 min), and the crystal growth kinetics might be well matched with the Avrami's hypothesis. However, secondary crystallization will be interfered because the PPy NPs act as a physical hindrance to crystal growth. The additional increment of crystal is not obvious, as shown in Figure 6.

The required time to reach the maximum degree of crystallinity is shorter in the PPy NP/PVA nanocomposite than pristine PVA. It means that the crystallization rate of PPy NP/PVA nanocomposite is fast comparing to the neat PVA. This result is also attributed to the efficient nucleation effect of PPy NPs in isothermal crystallization process.

The role of PPy NPs in crystallization process as a nucleating agent is also confirmed by DSC analysis. Figure 7(a) indicates the DSC thermograms of PVA and PPy/PVA nanocomposite at cooling rate of 10 °C/min. The crystallization exothermic peaks are observed in the range of 200~140 °C. The initial cooling crystallization temperature of nanocomposite has higher value than that of pristine PVA. The relative crystallinity as a function of time, $X(t)$, can be obtained from relative crystallinity as a function of temperature, $X(T)$, by transforming the temperature to a time scale along with the following equation:[4]

$$t = (T_i - T)/|C| \quad (1)$$

where C is cooling rate, T is temperature and T_i is the initial temperature when crystallization begins. The fraction of the polymer crystallized, $X(t)$, of pristine PVA and PPy NP/PVA (1 wt%) nanocomposite was presented in Figure 7(b). The time ($t_{1/2}$), at which half crystallization occurs, of pristine PVA and nanocomposite is about 1.18 and 0.97 min, respectively. Due to the heterogeneous nucleation effect of PPy nanoparticles, the crystallization rate of nanocomposite is faster than that of pristine PVA.

The crystallization kinetics was generally investigated using the following Avrami equation:[45,46]

$$X(t) = 1 - \exp[-k(t - t_{initial})^n] \quad (2)$$

where k is the overall kinetic constant, t is the time, $t_{initial}$ is the initial time of the crystallization process, and n is the Avrami exponent. Because the Avrami hypothesis is related

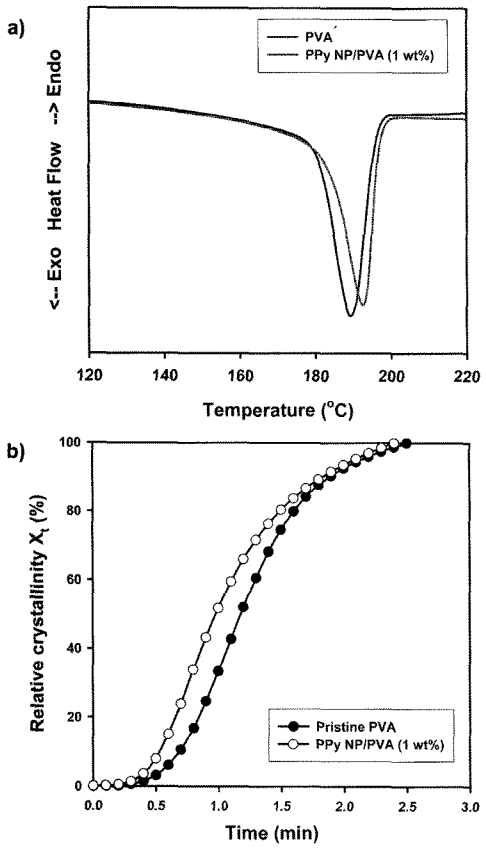

Figure 7. (a) DSC thermograms of PVA and PPy NP/PVA (1 wt%) cooled from 240 °C at cooling rate of 10 °C/min and (b) development of relative crystallinity, X_t, as a function of time in pristine PVA and PPy NP/PVA (1 wt%) nanocomposite.

with the isothermal crystallization, Ozawa equation is proposed to analyze non-isothermal process, by incorporating the cooling rate term, as following:[47]

$$1-X_T = \exp[-R(T)/C^m] \quad (3)$$

where X_T is the temperature-dependent relative crystallinity, $R(T)$ is the kinetic parameter at temperature T, C is the cooling rate, and m is Ozawa exponent. Eq. (3) can be transformed to following equation using eq. (1):[4]

$$\ln[-\ln(1-X_T)] = \ln R(T) - m \ln C = \ln k + n \ln t \quad (4)$$

Here, n and k values are directly connected with the coefficient of Avrami equation. Figure 8 shows the plot of $\ln[-\ln(1-X_T)]$ versus $\ln t$ for PVA and PPy/PVA nanocomposite (1 wt%). The values of n, k, and $t_{1/2}$ are summarized in Table II. As illustrated in Figure 8, the plot presents a linear tendency. The deviation from linear behavior at high conversions can be attributed to secondary crystallization phenomena.

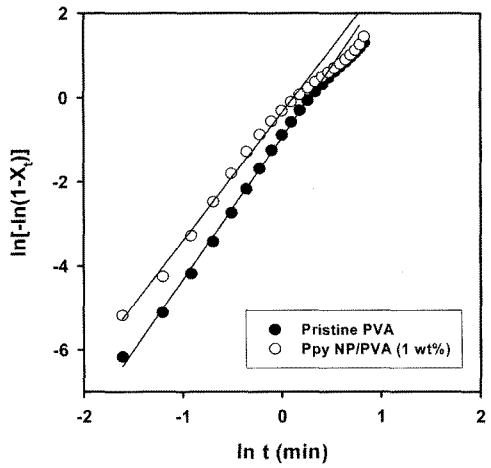

Figure 8. Plots of $\ln[-\ln(1-X_t)]$ versus $\ln t$ for PVA and PPy NP/PVA (1 wt%) nanocomposite.

Table II. Values of n, k, and $t_{1/2}$ at PVA and PPy NP/PVA Nanocomposite (1 wt%)

	PVA	PPy/PVA (1 wt%)
n	3.38	3.05
k	0.38	0.69
$t_{1/2}$	1.18	0.97

The n value of nanocomposite is smaller than that of pristine PVA, indicating that the nanocomposite undergoes PPy NP induced-heterogeneous nucleation. This result can be strong evidence that the amorphous PPy NPs can act as a role in effective nucleating agent in PVA matrix. In addition, the value k of nanocomposite has also higher values than that of pristine PVA, implying faster crystallization rate of the nanocomposite.

Conclusions

The PPy NP/PVA nanocomposite with various contents of PPy NP was successfully fabricated without particle aggregation. The crystallization behavior of neat PVA and PPy NP/PVA nanocomposite was investigated by FTIR, DSC, XRD and POM analysis. The PPy NPs acted as a nucleating agent of PVA crystallization at low filler contents (~1 wt%) and the addition of nanosized amorphous polymer could enhance the crystallinity of semi-crystalline polymer. Crystallization kinetic analysis indicated that the PPy nanoparticles played a role of the heterogeneous nucleating agent in PVA crystallization, leading to increase the degree of crystallinity and crystallization rate. In addition, the enhancement of degree of crystallinity for PVA nanocomposite was also confirmed using POM and XRD analysis.

Acknowledgement. This work has supported by by a grant from the Center for Advanced Materials Processing (CAMP) of the 21st Century Frontier R&D Program funded by the Ministry of Commerce, Industry and Energy (MOCIE), Republic of Korea.

References

(1) L. Pan, K. Y. Zhang, Y. G. Li, S. Q. Bo, and Y. S. Li, *J. Appl. Polym. Sci.*, **104**, 4188 (2007).
(2) J. Yu, D. Zhou, W. Chai, B. Lee, S. W. Lee, J. Yoon, and M. Ree, *Macromol. Res.*, **11**, 25 (2003).
(3) Z. Zhao, W. Zheng, W. Yu, H. Tian, and H. Li, *Macromol. Rapid Commun.*, **25**, 1340 (2004).
(4) T. M. Wu, S. F. Hsu, C. F. Chien, and J. Y. Wu, *Polym. Eng. Sci.*, **44**, 2288 (2004).
(5) C. Marega, V. Causin, and A. Marigo, *Macromol. Res.*, **14**, 588 (2006).
(6) M. O. Ngui and S. K. Mallapragada, *J. Polym. Sci. Part B: Polym. Phys.*, **36**, 2771 (1998).
(7) N. A. Peppas, *Makromol. Chem.*, **178**, 595 (1977).
(8) P.-D. Hong, C.-M. Chou, and W.-T. Chuang, *J. Appl. Polym. Sci.*, **79**, 1113 (2001).
(9) N. A. Peppas and P. J. Hansen, *J. Appl. Polym. Sci.*, **27**, 4787 (1982).
(10) J. F. Kenney and G. W. Willcockson, *J. Polym. Sci. Part A: Polym. Chem.*, **4**, 679 (1966).
(11) J. Lee, K. J. Lee, and J. Jang, *Polym. Testing*, **27**, 360 (2008).
(12) J. Won, S. M. Ahn, H. D. Cho, J. Y. Ryu, H. Y. Ha, and Y. S. Kang, *Macromol. Res.*, **15**, 459 (2007).
(13) S. D. Moon, Y. S. Kang, and D. J. Lee, *Macromol. Res.*, **15**, 491 (2007).
(14) J. K. Yun, H. J. Yoo, and H. D. Kim, *Macromol. Res.*, **15**, 22 (2007).
(15) H. Byun, B. Hong, S. Y. Nam, S. Y. Jung, J. W. Rhim, S. B. Lee, and G. Y. Moon, *Macromol. Res.*, **16**, 189 (2008).
(16) J. Jang, J. H. Oh, and S. I. Moon, *Macromolecules*, **33**, 1864 (2000).
(17) H. Sato, R. Murakami, J. Zhang, Y. Ozaki, K. Mori, I. Takahashi, H. Terauchi, and I. Noda, *Marcromol. Res.*, **14**, 499 (2006).
(18) K. Tashiro and H. Hama, *Macromol. Res.*, **12**, 1 (2004).
(19) A. Dasari, Z.-Z. Yu, and Y.-W. Mai, *Macromolecules*, **40**, 123 (2007).
(20) Y. H. Shin, W. D. Lee, and S. S. Im, *Macromol. Res.*, **15**, 662 (2007).
(21) J. Cai, Q. Yu, Y. Han, X. Zhang, and L. Jiang, *Eur. Polym. J.*, **43**, 2866 (2007).
(22) Z. Liu, K. Chen, and D. Yan, *Eur. Polym. J.*, **39**, 2359 (2003).
(23) Q. Yuan, S. Awate, and R. D. K. Misra, *Eur. Polym. J.*, **42**, 1994 (2006).
(24) X. Liu and Q. Wu, *Eur. Polym. J.*, **38**, 1383 (2002).
(25) J. Y. Kim, S. H. Kim, S. W. Kang, J.-H. Chang, and S. H. Ahn, *Macromol. Res.*, **14**, 146 (2006).
(26) K. Nie, S. Zheng, F. Lu, and Q. Zhu, *J. Polym. Sci. Part B: Polym. Phys.*, **43**, 2594 (2005).
(27) X. Tian, C. Ruan, P. Cui, W. Liu, J. Zheng, X. Zhang, X. Yao, K. Zheng, and Y. Li, *J. Macromol. Sci. Part B*, **45**, 835 (2006).
(28) L. Li, C. Y. Li, C. Ni, L. Rong, B. Hsiao, Z. Peng, L. X. Kong, and S.-D. Li, *Polymer*, **48**, 3452 (2007).
(29) J. Li, Z. Fang, L. Tong, A. Gu, and F. Liu, *Eur. Polym. J.*, **42**, 3230 (2006).
(30) M. L. Minus, H. G. Chae, and S. Kumar, *Polymer*, **47**, 3705 (2006).
(31) M. Joshi and B. S. Butola, *Polymer*, **45**, 4953 (2004).
(32) Y.-C. Ke, T.-B. Wu, and Y.-F. Xia, *Polymer*, **48**, 3324 (2007).
(33) J. Jang and K. Sim, *Polymer*, **38**, 4043 (1997).
(34) J. Jang and J. Won, *Polymer*, **39**, 4335 (1998).
(35) W. J. Bae, W. H. Jo, and Y. H. Park, *Macromol. Res.*, **10**, 145 (2002).
(36) H.-L. Wang and J. E. Fernandez, *Macromolecules*, **26**, 3336 (1993).
(37) S. P. Armes, J. F. Miller, and B. Vincent, *J. Colloid Interf. Sci.*, **118**, 410 (1987).
(38) S. P. Armes and B. Vincent, *J. Chem. Soc. Chem. Commun.*, 288 (1987).
(39) K. Ishizu, H. Tanaka, R. Saito, T. Maruyama, and T. Yamamoto, *Polymer*, **37**, 863 (1996).
(40) Y. Li, K. G. Neoh, and E. T. Kang, *J. Biomed. Mater. Res. Part A*, **73A**, 171 (2005).
(41) H. G. N. Kumar, J. L. Rao, N. O. Gopal, K. V. Narasimhulu, R. P. S. Chakradhar, and A. V. Rajulu, *Polymer*, **45**, 5407 (2004).
(42) T. Ohta, N. Shigemitsu, K. Suzuki, and T. Hashimoto, *Polymer*, **42**, 2201 (2001).
(43) H. S. Mansur, R. L. Orefice, and A. A. P. Mansur, *Polymer*, **45**, 7193 (2004).
(44) Y.-H. Yu, C.-Y. Lin, J.-M. Yeh, and W.-H. Lin, *Polymer*, **44**, 3553 (2003).
(45) M. Avrami, *J. Chem. Phys.*, **7**, 1103 (1939).
(46) M. Avrami, *J. Chem. Phys.*, **8**, 212 (1940).
(47) T. Ozawa, *Polymer*, **12**, 150 (1971).